Physiological and Molecular Characterization of a *Synechocystis* sp. PCC 6803 Mutant Lacking Histidine Kinase Slr1759 and Response Regulator Slr1760

Anke Nodop[a], Iwane Suzuki[b,d], Aiko Barsch[c], Ann-Kristin Schröder[a], Karsten Niehaus[c], Dorothee Staiger[a], Elfriede K. Pistorius[a], and Klaus-Peter Michel[a,*]

[a] Universität Bielefeld, Biologie VIII: Molekulare Zellphysiologie, D-33501 Bielefeld, Germany. E-mail: klauspeter.michel@uni-bielefeld.de
[b] Division of Cellular Regulation, National Institute for Basic Biology, Myodaiji, Okazaki 444-8585, Japan
[c] Universität Bielefeld, Biologie VI: Genetik, D-33501 Bielefeld, Germany
[d] Present address: Graduate School of Life and Environmental Sciences, University of Tsukuba, Tsukuba, Ibaraki 305-8572, Japan

* Author for correspondence and reprint requests

Z. Naturforsch. **61c**, 865–878 (2006); received June 6/30, 2006

The hybrid sensory histidine kinase Slr1759 of the cyanobacterium *Synechocystis* sp. strain PCC 6803 contains multiple sensory domains and a multi-step phosphorelay system. Immuno blot analysis provided evidence that the histidine kinase Slr1759 is associated with the cytoplasmic membrane. The gene *slr1759* is part of an operon together with *slr1760*, encoding a response regulator. A comparative investigation was performed on *Synechocystis* sp. strain PCC 6803 wild type (WT) and an insertionally inactivated *slr1759*-mutant (Hik14) which also lacks the transcript for the response regulator Slr1760. The mutant Hik14 grew significantly slower than WT in the early growth phase, when both were inoculated with a low cell density into BG11 medium without additional buffer and when aerated with air enriched with 2% CO_2. Since the aeration with CO_2-enriched air results in a decrease of the pH value in the medium, the growth experiments indicated that Hik14 is not able to adjust its metabolic activities as rapidly as WT to compensate for a larger decrease of the pH value in the medium. No significant differences in growth between Hik14 and WT were observed when cells were inoculated with a higher cell density in BG11 medium or when the BG11 medium contained 50 mM Epps-NaOH, pH 7.5, to prevent the pH drop. This Hik14 phenotype has so far only been seen under the above defined growth condition. Results of photosynthetic activity measurements as well as Northern blot-, immuno blot-, and metabolite analyses suggest that the two-component system Slr1759/Slr1760 has a function in the coordination of several metabolic activities which is in good agreement with the complex domain structure of Slr1759. The direct targets of this two-component system have so far not been identified.

Key words: Synechocystis sp. PCC 6803, Two-Component System, Histidine Kinase

Introduction

Like other prokaryotes, cyanobacteria are able to monitor the environment and to adjust their growth and metabolism in response to the physicochemical parameters of their habitat. Signal transduction networks involved in these processes frequently consist of "two-component systems" (Chang and Stewart, 1998; Galperin, 2004; Stock *et al*., 2000) harboring a sensor kinase and a cognate response regulator. After publication of the genome sequence of *Synechocystis* sp. PCC 6803 (Kaneko *et al.*, 1996) a computer-assisted similarity search of the genome identified 92 ORFs with significant similarity to known two-component signal transducers from other bacterial species (Kaneko *et al*., 2003; Mizuno *et al.*, 1996; Murata and Suzuki, 2006; West and Stock, 2001). Among these, 47 ORFs encode putative sensory histidine kinases (44 ORFs are located on the chromosome, 3 ORFs are located on plasmids) and 45 ORFs encode response regulators. For a number of these two-component modules a specific function in a wide range of adaptive processes in response to external and/or internal signals in *Synechocystis*

Abbreviations: Chl, chlorophyll; PS, photosystem; Hik14, Slr1759-free and Slr1760-free *Synechocystis* sp. PCC 6803 mutant; WT, wild type.

0939–5075/2006/1100–0865 $ 06.00

sp. PCC 6803 has been elucidated (Murata and Suzuki, 2006 and references therein).

In prokaryotes, PAS domains (Taylor and Zhulin, 1999; Zhulin *et al.*, 1997) frequently serve as input domains for sensory histidine kinases sensing redox changes in the photosynthetic and respiratory electron transport system or in the overall cellular redox status. As suggested by Zhulin and Taylor (1998), there seems to be a positive correlation between the number of PAS domains and the number of electron transport-associated proteins in several species. *Synechocystis* sp. PCC 6803, whose survival is dependent on sensing light and the redox status of the photosynthetic and respiratory electron transport chains, is an organism with a high abundance of PAS domains (Zhulin *et al.*, 1997).

Many questions regarding the complex interrelationship between respiration and photosynthesis in cyanobacteria have so far remained unanswered (Hirano *et al.*, 1980; Vermaas, 2001). It is still unclear how many different routes exist for PS I-mediated cyclic electron transport (Howitt *et al.*, 2001; Matthijs *et al.*, 2002; Yeremenko *et al*., 2005 and references therein). It has also been shown that the NDH-1 complex exists in multiple forms (Herranen *et al*., 2004; Ohkawa *et al.*, 2000, 2002; Prommeenate *et al*., 2004). As Ohkawa *et al.* (2002) defined, the NDH-1A complexes contain either NdhD1 or NdhD2, while NDH-1B complexes contain either NdhD3 or NdhD4. The latter complexes have a function in CO_2 to HCO_3^- conversion. Moreover, the direct substrate for these complexes has not yet been identified (Berger *et al.*, 1993; Friedrich and Scheide, 2000). Since Ohkawa *et al.* (2001) were not able to detect the NDH-1 complex in the cytoplasmic membrane of *Synechocystis* sp. PCC 6803, the first complex of the respiratory electron transport chain in the cytoplasmic membrane is still unidentified. Moreover, the finding that the uptake of inorganic carbon is directly linked to the electron transport activity, adds another level of complexity to the overall network of cyanobacterial electron transport activities (Badger *et al.*, 2002; Badger and Price, 2003; Kaplan and Reinhold, 1999; Ogawa and Kaplan, 2003).

In this paper we have used a bioinformatic approach to select a histidine kinase which is membrane-associated and has domains capable of redox regulation, and thus, could be a likely candidate to have a function in the coordination of the carbon metabolism in *Synechocystis* sp. PCC 6803.

Materials and Methods

Cyanobacterial strains

Synechocystis sp. strain PCC 6803 (hereafter referred to as *Synechocystis* PCC 6803) wild type (WT) and its Slr1759/Slr1760-free mutant derivative (Suzuki *et al.*, 2000) were obtained from the laboratory of Prof. Dr. N. Murata (National Institute for Basic Biology, Okazaki, Japan, via Prof. Dr. M. Hagemann, Universität Rostock, Germany). The WT is the glucose-tolerant strain and originates from Prof. Dr. J. G. K. Williams (Du Pont de Nemours & Co. Inc., Wilmington, DE, USA). The Slr1759/Slr1760-free *Synechocystis* PCC 6803 mutant (Hik14) contains a spectinomycin resistance cassette in the gene *slr1759* in position bp 534592 on the chromosome and is fully segregated (not shown) (Suzuki *et al.*, 2000).

Growth conditions and preparation of cell suspensions

Synechocystis PCC 6803 was basically grown as described by Stephan *et al.* (2000). The bottles (250 mL) were placed in a water bath of 30 °C and illuminated with Philips lamps (Cool Spot, $\measuredangle$ 12°, 150 W) resulting either in 200 μmol photons m^{-2} s^{-1} or 60 μmol photons m^{-2} s^{-1}. The light intensity was determined with a LI-250 Light Meter with a LI-190SZ Quantum Sensor (Li-COR, Lincoln, NB, USA) measuring photons between 400 to 700 nm. The cells were cultivated in BG11 medium containing either no additional buffer or 50 mM Epps [4-(2-hydroxyethyl)-1-piperazinepropanesulfonic acid]-NaOH, pH 7. 5. For growth of the Slr1759/Slr1760-free mutant spectinomycin was added at a concentration of 20 mg L^{-1}. In general, the medium was bubbled via two manometers (Porter Instruments, Hatfield, USA) with 20 L h^{-1} 2% CO_2-enriched air. The pH value of the autoclaved BG11 medium dropped from about 7.5 to about 6.6 (pH value in absence of cells) when bubbled with air enriched with 2% CO_2. In contrast, the pH value remained almost constant when 50 mM Epps-NaOH, pH 7.5, was added to the BG11 medium. Cells were inoculated with a cell density as given in the legends to the figures/tables and were in general grown for 2 or 3 d as indicated. Cyanobacterial growth was determined by measuring the optical density at 750 nm ($OD_{750\,nm}$). For inoculation cells were harvested

by centrifugation and resuspended in a small amount of medium.

For preparation of cell suspensions, *Synechocystis* cells were harvested by centrifugation for 30 min at $2{,}200 \times g$ and then resuspended in the growth medium to give a cell density corresponding to an $OD_{750\,nm}$ of 100.

Biochemical determinations

Protein content and chlorophyll content were determined as previously described (Tölle *et al.*, 2002).

Photosynthetic O_2 evolution of cell suspensions was determined in a Clark-type electrode at 30 °C as described by Stephan *et al.* (2000). The reaction mixture of 3 mL contained BG11 medium, 15 mM $NaHCO_3$, and cell suspension corresponding to 5 to 15 μg chlorophyll (Chl). The reaction chamber was illuminated with red light of 200 μmol photons $m^{-2}\,s^{-1}$. Light was filtered through a glass cuvette containing 2% Cu_2SO_4 solution and a red Plexiglas filter (RG1–610, Schott, Mainz, Germany).

Measurement of pigment fluorescence at 77 K

S*ynechocystis* PCC 6803 cells were adjusted to a Chl concentration in the range of 1 to 10 μg Chl mL^{-1} by dilution with the corresponding growth medium, then transferred to cryotubes and immediately frozen in liquid nitrogen. Fluorescence emission spectra were recorded at 77 K in a Perkin-Elmer luminescence spectrometer LS50B with excitation at 435 nm (± 10 nm) or 600 nm (± 10 nm) over an emission range of 630 nm or 670 nm to 750 nm (± 5 nm, 515 nm cut-off filter) and at a speed of 200 nm min^{-1}. The emission peak at 685 nm corresponds to the fluorescence of the phycobilisome terminal emitter and the small Chl a antenna of PS II (CP43), the fluorescence at 695 nm is emitted by CP47 and P_{680} of functional PS II centers, and the peak at 725 nm represents PS I-related fluorescence. Emission in the 660 nm region corresponds to the fluorescence of the phycobilisome antenna (Meunier *et al.*, 1997; Mullineaux and Allen, 1990).

SDS-PAGE and immuno blotting

SDS-PAGE and immuno blotting were performed as previously described (Tölle *et al.*, 2002). Cells were harvested by centrifugation, resuspended in 50 mM Tris-HCl, pH 7.4, containing 5 mM EDTA-NaOH, pH 7.4, 1 mM benzamidine, 0.1 mM PMSF, and broken in a Hybaid Ribolyser (FastPrep Instrument, Q-biogene, Heidelberg, Germany). The extract was centrifuged for 1 min at $16{,}200 \times g$ at 4 °C, and the supernatant was used. Samples corresponding to 15 μg proteins were denatured for 20 min at 60 °C using a dithiothreitol- and SDS-containing buffer and subjected to Tris-glycine SDS-PAGE. Subsequently, the proteins were transferred to BA-85S nitrocellulose membranes (Schleicher and Schuell, Dassel, Germany) as described previously (Michel *et al.*, 1996). The antisera used were: anti-Lpd antiserum (Engels *et al.*, 1997), anti-PsbA, anti-PsbO, and anti-AtpA antiserum (Tölle *et al.*, 2002) as well as anti-PsaA/B antiserum (kind gift of Dr. Kruip, Lehrstuhl für Biochemie der Pflanzen, Ruhr-Universität Bochum, Germany). The anti-Slr1759 antiserum was raised in rabbits against two intrinsic synthetic peptides of 20 and 19 amino acids length. Both peptides were coupled via an additional extrinsic cysteine residue to keyhole limpet haemocyanin (Pineda Antikörper-Service, Berlin, Germany). The second antibody was a peroxidase-coupled swine anti-rabbit IgG (dilution 1 to 250–500) or an alkaline phosphatase-conjugated goat anti-rabbit IgG (dilution 1 to 500; DAKO A/S, Glostrup, Denmark). Immuno blot staining was performed either with the ECL detection kit (GE Healthcare, Munich, Germany) or with nitrotetrazolium blue/X-phosphate as substrate for the alkaline phosphatase.

Isolation of total RNA, Northern blot analysis, and RT-PCR

Synechocystis PCC 6803 cultures were harvested with crushed ice at the times indicated in the figures. Total RNA was isolated using a hot acidic phenol extraction procedure (Reddy *et al.*, 1990) and the RNeasy kit (Qiagen, Hilden, Germany). The aqueous phase resulting from the phenol extraction was applied to spin-through columns of the kit for further purification. For hybridization experiments, 5 or 10 μg RNA were denatured at 68 °C in a formaldehyde/formamide-containing buffer and separated in a formaldehyde-containing 1.3% agarose gel (Michel *et al.*, 1999). After capillary transfer to HybondN$^+$ membranes (Amersham Pharmacia Biotech, Freiburg, Germany), RNA was UV cross-linked to the membrane and samples were probed with different PCR-derived digoxygenin-dUTP-labeled (Dig-dUTP) gene-specific probes. PCR with specific primers was carried out using the *Taq* polymerase kit (Qiagen) and

Table I. Primers utilized for Northern blot hybridization and RT-PCR.

Primers utilized for Northern blot hybridization Gene (encoded protein)	Gene number	Sequence in 5′→3′ direction
ndhH (NADH dehydrogenase subunit 7)	*slr0261*	TATGCACGGGGTGTTACGTT GTCCACCGATCCCATGATAA
ndhD1 (NADH dehydrogenase subunit 4)	*slr0331*	TGTGGCGGCTTTATTCATTC TGACTTCCAAGGGTGAAAGG
ndhD2 (NADH dehydrogenase subunit 4)	*slr1291*	TCCGTTAATTCCCGACAAAG GGAATGTGGGGAGCAGTTAAT
ndhD3 (NADH dehydrogenase subunit 4)	*sll1733*	CCTGCCAGTTATCGGAGCTT ACCAGATGGAACAGCAGAG
ndhD4 (NADH dehydrogenase subunit 4)	*sll0027*	CAATGATGACCACCGCCAAG TCCACACCTGGCTACCGGAT
petH (Ferredoxin:NADP oxidoreductase)	*slr1643*	ATGTACAGTCCCGGTTACGTAG TTAGTAGGTTTCCACGTGCCAG
rnpB (RNase P catalytic RNA)	*rnpB*	GCGGCCTATGGCTCTAATCA TTGACAGCATGCCACTGGAC
Primers utilized for RT-PCR **Gene**	**Primer**	**Sequence in 5′→3′ direction**
slr1759	*slr1759-forward*	GGCGCACCATCTACGACAAT
	slr1759-reverse	GCGTAATCAGCCAGACCTATAGACC
slr1760	*slr1760-forward*	TACAACAGGTGGCTAAGGCT
	slr1760-reverse	GGTAATCTCCGCCTGGATGTCTTCA
slr1761	*slr1761-forward*	GAGGCGGCCAGTGTAGTGTACTTCT
	slr1761-reverse	TATTGTCACCACCGAGTCTG

substitution of one-tenth of the regular dTTP concentration with Dig-dUTP (Roche Molecular Biochemicals, Mannheim, Germany). Northern blots were developed according to the manufacturer's recommendation. The primers used in the experiments of Fig. 7 are listed in Table I. The *rnpB* probe was used in all experiments to assure equal loading of total RNA.

The preparation of RNA samples for the reverse transcription assay included a cartridge-based DNase digestion step with the RNase-free DNase kit from Qiagen according to the manufacturer's recommendations. The reverse transcription of 5 μg total RNA was carried out with SuperscriptII-RT (Invitrogen, Karlsruhe, Germany) and gene specific primers (listed in Table I) following the manufacturer's recommendation. 2 μL out of the 20 μL RT assay were then used as cDNA template for the PCR with the corresponding primers (listed in Table I). The primers were designed to generate PCR products of 189, 152, and 106 bp sizes for *slr1759*, *slr1760*, and *slr1761*, respectively. Absence of residual genomic DNA template in the RNA samples used for RT-PCR has been tested for each assay using a mock RT assay without SuperscriptII-RT followed by the PCR assay.

Metabolite profiling

Approximately 50 mL *Synechocystis* PCC 6803 cell suspension were harvested by filtration through a nylon membrane (pore size 0.45 μm; Sigma-Aldrich, Deisenhofen, Germany) using a vacuum manifold. The cells were rapidly removed from the filter and frozen in liquid nitrogen. After lyophilization 1 to 10 mg cells were used for the subsequent analyses. Determination of the relative concentration of hydrophilic metabolites in the cells was the same as described by Barsch *et al.* (2004). The numbers given in Table III are relative

units which allow for comparison of identical substances in the investigated samples. The relative units of different substances can not directly be compared with each other.

Bioinformatic analysis

Bioinformatic analyses to identify putative domains were performed using the following programs: SMART Sequence (http://smart.embl-heidelberg.de/), Pfam Motif Search, http://pfam.wustl.edu), TMHMM predict (http://www.cbs.dtu.dk/services/TMHMM-2.0/), TM pred (http://www.ch.embnet.org/software/TMPRED_form.html), InterProScan (EMBL-EBI, http://www.ebi.ac.uk/InterProScan/).

Results

Selection of the histidine kinase Slr1759 as a likely candidate for coordinating carbon metabolism in Synechocystis PCC 6803

The following criteria were applied for selecting Slr1759 in *Synechocystis* PCC 6803 as a histidine kinase which might have a function in the coordination of carbon metabolism in response to the redox state of the cytoplasmic or thylakoid membrane located electron transport chains: Previous investigations have shown that *Synechocystis* PCC 6803 contains 47 putative histidine kinase encoding genes (Murata and Suzuki, 2006). The evaluation by Taylor and Zhulin (Taylor and Zhulin, 1999; Zhulin *et al.*, 1997) indicated that *Synechocystis* PCC 6803 contains at least 17 proteins with one or several PAS domains. According to a recent evaluation with the SMART Sequence software (unpublished results) among the 47 sensory histidine kinases 14 kinases possess a putative PAS domain(s). We selected Slr1759, because it has two transmembrane helices and two PAS domains with two associated PAC domains in the *N*-terminal region, making the enzyme a good candidate for a membrane-anchored histidine kinase sensing the redox state of the membrane. The entire putative domain structure of the hybrid sensory kinase Slr1759 is presented in Fig. 1A (p. 871).

Slr1759 consists of 1462 amino acids resulting in a molecular mass of 163.9 kDa and has a calculated pI of 5.06. Slr1759 contains a HIS_KIN domain consisting of a histidine kinase A domain (SIG A) with the conserved histidine residue and an ATP-binding domain (HATPase_C) (Fig. 1A). In the *N*-terminal region, the enzyme possesses two transmembrane helices separated by 240 amino acid residues. 54 of these amino acid residues can be protonated or deprotonated in dependence of the pH value of the periplasm. A CHASE domain, which represents an extracellular sensory domain (Anantharaman and Aravind, 2001; Mougel and Zhulin, 2001; Zhulin *et al.*, 2003), is predicted between the two transmembrane helices. Slr1759 also contains two PAS/PAC domains followed by a GAF domain. Since Slr1759 possesses multiple putative sensory domains, it should be able to sense more than one signal.

In the *C*-terminal region, the enzyme possesses two response regulator domains and an additional histidine-containing phosphotransfer domain (Hpt), which is found in a number of signal transducers (Matsushika and Mizuno, 1998 and references therein). Thus, Slr1759 belongs to the group of hybrid histidine kinases with a multi-step phosphorelay system which may have multiple regulatory functions and which may also provide junction points for communication with other signaling pathways (Appleby *et al.*, 1996).

Slr1759 shows the highest similarity to the hybrid histidine kinase BarA of *E. coli* (918 amino acids, molecular mass 102 kDa, pI 5.41) which also contains a Hpt domain (Pernestig *et al.*, 2003). The identity of the *C*-terminus of Slr1759 (aa 730–1453) with that of BarA (aa 247–918) is 30.6%, and the similarity corresponds to 48.8%. However BarA does not possess a CHASE domain, a PAS/PAC domain or a GAF domain. Recently, it has been shown that the BarA-UvrY two-component system is crucial for efficient adaptation to different carbohydrate-metabolizing pathways under rapidly changing environmental conditions (Pernestig *et al.*, 2003).

Immediately downstream of the histidine kinase encoding gene *slr1759*, the gene *slr1760*, encoding a putative response regulator (Mizuno *et al.*, 1996), and the gene *slr1761*, encoding a protein of 12 kDa with similarity to peptidyl-prolyl *cis-trans* isomerases, are located (see Fig. 2A (p. 871)). Since all three genes overlap by three nucleotides, it is likely that two or all three of them are co-transcribed. This is indeed the case for the genes s*lr1759* and *slr1760* but not for the gene *slr1761* as shown below (Fig. 2A). Thus, it can be assumed that Slr1759 and Slr1760 represent the corresponding sensor-regulator pair being located in the same transcriptional unit. The response regulator Slr1760 has a calcu-

lated molecular mass of 35.48 kDa and a pI of 5.51 (Fig. 1B). It contains the invariant aspartate residue in the receiver domain followed by a GGDEF domain. This domain has similarity to the adenylyl cyclase catalytic domain with diguanylate cyclase activity.

Characteristics of the Synechocystis PCC 6803 mutant Hik14

For a functional analysis of the histidine kinase Slr1759, we obtained a *Synechocystis* PCC 6803 mutant (Hik14) from the laboratory of Prof. Murata. Since analysis of the nucleotide sequence downstream of *slr1759* indicated that the gene *slr1759* and the gene *slr1760,* and possibly also the gene *slr1761* could be located in an operon (Fig. 2A), the transcript level of these three genes was investigated by RT-PCR (Fig. 2B). These investigations showed that the insertionally inactivated *slr1759* mutant does not contain transcripts for *slr1759* and for *slr1760*. However, it contains the transcript for *slr1761*. Thus, the mutant Hik14 presumably lacks both, the histidine kinase Slr1759 and the response regulator Slr1760. On the basis of these results, it can be suggested that *slr1759* and *slr1760* are located in a transcriptional unit, are co-transcribed, and the proteins Slr1759 and Slr1760 represent a classical two-component system encoded by two genes being arranged in tandem.

This conclusion is supported by results of a two-hybrid analysis (Kaneko *et al.*, 2005) in which both proteins interacted. However, this finding does not exclude that Slr1759 might also interact with additional response regulators.

Localization of the histidine kinase Slr1759

An anti-Slr1759 antiserum was raised against two synthetic intrinsic peptides consisting of 20 and 19 aa length representing aa 81–100 and 301–319 of the histidine kinase, respectively. This antiserum detected the histidine kinase in *Synechocystis* PCC 6803 WT and proved its absence in the mutant Hik14 (Fig. 3A). To investigate the subcellular localization of Slr1759, cytoplasmic membranes of *Synechocystis* PCC 6803 were isolated according to the procedure given in Omata and Murata (1984). Immuno blot analysis detected Slr1759 in the isolated cytoplasmic membrane fraction (Fig. 3C). Therefore, we concluded that this histidine kinase is a cytoplasmic membrane-anchored enzyme – a conclusion which is in line with the presence of two predicted transmembrane helices and a long CHASE domain in the *N*-terminal region (Fig. 1A).

Identification of growth conditions leading to a difference in growth between Synechocystis PCC 6803 WT and the mutant Hik14

Synechocystis PCC 6803 WT and mutant Hik14 were cultivated either with light of 200 μmol photons m^{-2} s^{-1} (experiments in Fig. 4, p. 872) to optimize the difference in growth between the two strains or with light of 60 μmol photons m^{-2} s^{-1} (all other experiments) to reduce secondary damaging effects as *e.g.* caused by photoinhibitory damage, especially under those conditions under which the mutant cells grew poorly in comparison to WT.

In the initial growth experiments (Fig. 4) *Synechocystis* PCC 6803 WT and mutant Hik14 cells were illuminated with 200 μmol photons m^{-2} s^{-1} and aerated with air enriched with 2% CO_2. Cells were inoculated in BG11 medium without or with 50 mM Epps-NaOH. The cell density ($OD_{750\,nm}$) at the time of inoculation was either 0.2 (Fig. 4, left) or 0.4 (Fig. 4, right). When inoculated with the higher cell density, Hik14 and WT showed an almost identical growth. However, when inoculated with the low cell density, Hik14 practically showed no growth over a period of six days in contrast to WT. This difference in growth between WT and mutant Hik14 was only detected in a rather narrow range of cell densities at the time of inoculation ($OD_{750\,nm}$ between 0.1 and 0.3) but was highly reproducible. The growth difference was detected in at least 10 independent experiments. Below an inoculation density of 0.1 growth of WT was also low (not shown).

When inoculated in BG11 medium buffered with 50 mM Epps-NaOH, pH 7.5, no difference in growth between Hik14 and WT was observed. Thus, the growth reduction of Hik14 relative to WT was only seen when the cells were inoculated with a low cell density into BG11 medium without additional buffer and when aerated with CO_2-enriched air (Fig. 4 left).

Aeration of autoclaved BG11 medium (pH 7.5) with air enriched with 2% CO_2 lowers the pH to about 6.6 unless the medium contains 50 mM Epps-NaOH. As can be seen in Fig. 4 (left), after 24 h of growth the pH value of the BG11 medium was 6.6 and 6.3 for WT and Hik14, respectively. Due to the metabolic activities, WT raised the pH value

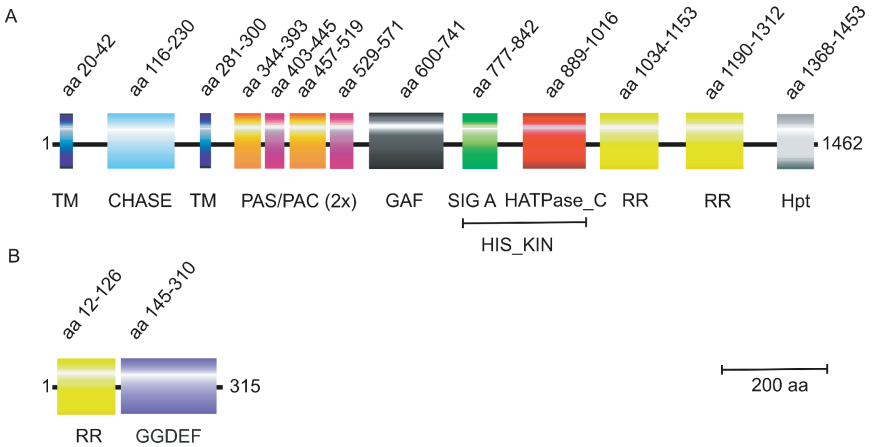

Fig. 1. (A) Predicted domain structure of the histidine kinase Slr1759 of *Synechocystis* PCC 6803 based on an analysis with the programs Pfam Motif Search and InterProScan. Transmembrane helices were identified using the programs TMHMM predict and TM pred. (B) Predicted domain structure of the response regulator Slr1760 of *Synechocystis* PCC 6803. Abbreviations as given in the figure from left to right: TM, transmembrane helix; CHASE, chase domain; PAS, PAS domain; PAC, PAC domain; GAF, GAF domain; HIS_KIN, histidine kinase A domain consisting of a SIG A and a HATPase_C ATP-binding domain; RR, response regulator; Hpt, phosphotransfer domain; GGDEF, GGDEF domain.

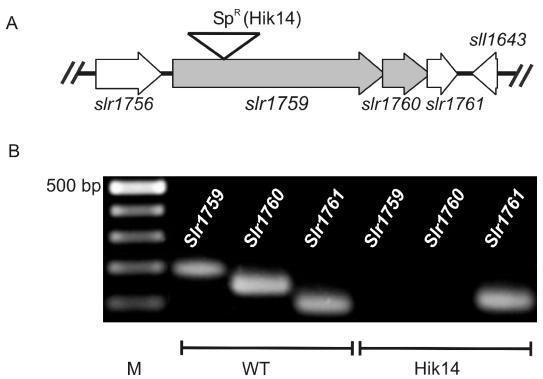

Fig. 2. Localization of the genes *slr1759* and *slr1760* on the chromosome of *Synechocystis* PCC 6803. *Slr1759* encodes the sensory hybrid histidine kinase and *slr1760* its corresponding response regulator. (A) *Slr1759* and *slr1760* represent a transcriptional unit and overlap by three nucleotides. The location of the spectinomycin resistance cassette in *slr1759* of mutant Hik14 is indicated by the triangle. (B) Detection of *slr1759*, *slr1760*, and *slr1761* transcripts by RT-PCR. All three transcripts are present in *Synechocystis* PCC 6803 WT, whereas *slr1759* and *slr1760* transcripts are absent in Hik14.

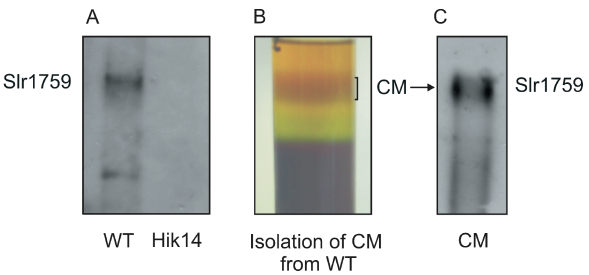

Fig. 3. Localization of the histidine kinase Slr1759. (A) The anti-Slr1759 antiserum detects the histidine kinase Slr1759 in *Synechocystis* PCC 6803 WT and proves its absence in the *Synechocystis* PCC 6803 mutant Hik14 in total cell extract. (B) Isolation of cytoplasmic membranes by sucrose gradient centrifugation. (C) Detection of the histidine kinase Slr1759 in the isolated cytoplasmic membrane fraction of *Synechocystis* PCC 6803 using the anti-Slr1759 antiserum. 75 μg of protein were resolved on a 12% SDS PAGE. The immuno blots were probed with an anti-Slr1759 antiserum. CM, cytoplasmic membrane fraction.

of the medium back to about pH 7 within 48 h of growth, while Hik14 did not raise the pH value during an entire growth phase of 96 h when cells were inoculated with a cell density of $OD_{750\,nm}$ of 0. 2. In contrast, when cells were inoculated with the higher cell density (Fig. 4, right), the changes in the pH value of the BG11 medium during the growth phase were about equal for Hik14 and WT, and both strains grew about equally well. The pH value of the 50 mM Epps-NaOH-buffered BG11 medium never dropped below pH 7.1 and remained between 7.1 and 7.4 over the entire growth phase (Fig. 4). In buffered BG11 medium Hik14 and WT grew equally well, independently whether inoculated with high or low cell density.

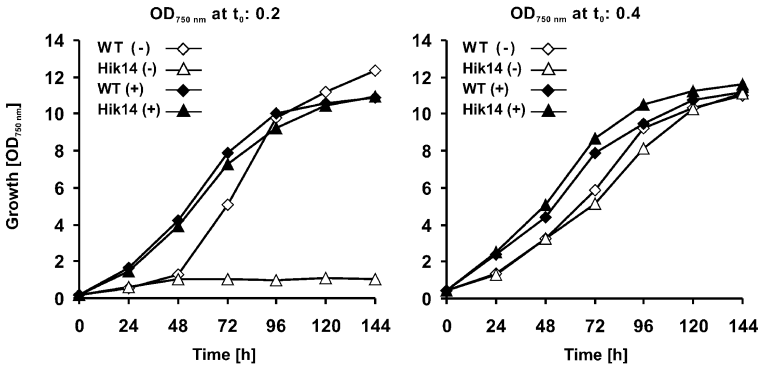

Growth [h]	0	24	48	72
	[pH of medium]			
- Epps: WT	7.1	6.6	7.0	7.2
- Epps: Hik14	7.1	6.3	6.5	6.5
+ Epps: WT	7.3	7.1	7.3	7.3
+ Epps: Hik14	7.3	7.1	7.2	7.2

Growth [h]	0	24	48	72
	[pH of medium]			
- Epps: WT	7.3	6.8	7.1	7.2
- Epps: Hik14	7.3	6.9	7.2	7.1
+ Epps: WT	7.3	7.3	7.4	7.4
+ Epps: Hik14	7.3	7.3	7.4	7.4

Fig. 4. Growth of *Synechocystis* PCC 6803 WT and Hik14 with an illumination of 200 μmol photons m^{-2} s^{-1}. The cells were grown with an illumination of 200 μmol photons m^{-2} s^{-1} and aerated with 2% CO_2-enriched air. Inoculation was with an $OD_{750\,nm}$ of 0.2 (left) or 0.4 (right): ◇ WT in BG11 medium without additional buffer; △ Hik14 in BG11 medium without additional buffer; ◆ WT in BG11 medium with Epps buffer; ▲ Hik14 in BG11 medium with Epps buffer. Absence or presence of Epps buffer is indicated as – or +, respectively, in the figure. Below the growth curves the pH value of the medium is given.

These results suggest that during growth *Synechocystis* PCC 6803 cells excrete OH^- and/or take up H^+ (or other basic or acidic substances) resulting in an alkalization of the medium. This is indeed the case as can be seen when *Synechocystis* cells are cultivated in BG11 medium without additional Epps buffer, illuminated with light of 200 μmol photons m^{-2} s^{-1}, and aerated with air without CO_2 supplementation (not shown). Under such conditions the pH value of the BG11 medium without Epps buffer went up from pH 7.6 to about pH 10 within 24 h of growth and remained high during the entire growth phase of 72 h. No significant difference in growth between Hik14 and WT was observed when cells were inoculated with a low cell density under these conditions ($OD_{750\,nm}$ of 0.2) (not shown).

To determine whether the difference between Hik14 and WT was also detectable when the light intensity was reduced, the experiments of Fig. 4 were repeated at a reduced light intensity of 60 μmol photons m^{-2} s^{-1} (Fig. 5). Again, Hik14 showed a significantly lower growth in the initial growth phase as compared to WT when cells were cultivated in BG11 medium (without additional Epps buffer), aerated with CO_2-enriched air, and inoculated with a low cell density ($OD_{750\,nm}$ of 0.1) (Fig. 5, left). However, in contrast to growth with an illumination of 200 μmol photons m^{-2} s^{-1} (Fig. 4, left), the mutant cells eventually started logarithmic growth within a period of about four to five days when grown with light of 60 μmol photons m^{-2} s^{-1} (Fig. 5, left). Thus, the difference between Hik14 and WT was mainly in the initial growth phase, before the pH value of the medium again reached a value of about 7 (Fig. 5, left). Therefore, the major difference is that the mutant cells required a substantially longer time, to start logarithmic growth which was then almost equal to WT growth. Thus, these growth conditions with an illumination of 60 μmol photons m^{-2} s^{-1} were better suited for further characterization of the mutant *vs.* WT.

Fig. 5 (right) also shows that when increasing the cell concentration at the time of inoculation, the phase with reduced growth was equal (about one day) for Hik14 and WT. In the later growth phase Hik14 even showed a slightly higher growth than WT. Thus, absence of Slr1759 can also result in a ~20% growth advantage for the mutant cells under defined conditions. When adding Epps buffer to the BG11 medium, again no significant

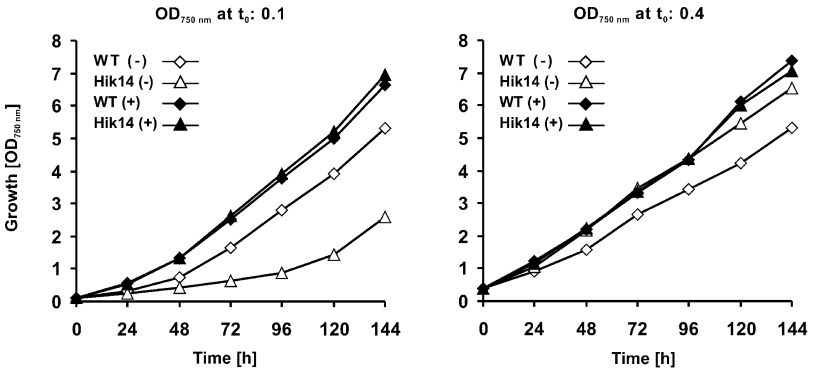

Growth [h]	0	24	48	72	96	100	144
	[pH of medium]						
- Epps: WT	7.1	6.4	6.9	7.2	7.4	7.5	7.7
- Epps: Hik14	7.1	6.3	6.7	6.8	7.0	7.2	7.4
+ Epps: WT	7.6	7.2	7.4	7.4	7.4	7.5	7.5
+ Epps: Hik14	7.6	7.2	7.3	7.4	7.4	7.5	7.5

Growth [h]	0	24	48	72	96	100	144
	[pH of medium]						
- Epps: WT	7.1	6.7	7.1	7.3	7.4	7.5	7.6
- Epps: Hik14	7.1	6.7	7.2	7.4	7.5	7.6	7.7
+ Epps: WT	7.6	7.2	7.4	7.4	7.4	7.5	7.5
+ Epps: Hik14	7.6	7.2	7.3	7.4	7.4	7.4	7.5

Fig. 5. Growth of *Synechocystis* PCC 6803 WT and Hik14 with an illumination of 60 μmol photons m^{-2} s^{-1}. The cells were grown with an illumination of 60 μmol photons m^{-2} s^{-1} and aerated with 2% CO_2-enriched air. Inoculation was with an $OD_{750\,nm}$ of 0.1 (left) or 0.4 (right): ◇ WT in BG11 medium without additional buffer; △ Hik14 in BG11 medium without additional buffer; ◆ WT in BG11 medium with Epps buffer; ▲ Hik14 in BG11 medium with Epps buffer. Absence or presence of Epps buffer is indicated as – or +, respectively, in the figure. Below the growth curves the pH value of the medium is given.

difference between Hik14 and WT was detectable whether inoculated with an $OD_{750\,nm}$ of 0.4 or 0.1 (Fig. 5).

Taken together, we provide evidence that the mutant Hik14 was not equally able like WT to rapidly compensate for a pH drop of the medium when inoculated with a low cell density. However, it should also be stated that the mutant phenotype is only seen under clearly defined growth conditions. The deviation was rather small or not existing under the majority of growth conditions (at least under those conditions so far tested). Deletion of other histidine kinases can also have rather subtle effects, see *e.g.* the results obtained with the BarA-free *E. coli* mutants (Pernestig *et al.*, 2003). This could be interpreted as a result of redundancy in regulatory cascades.

Comparison of the photosynthetic activity of WT and Hik14

For the identification of differences in metabolic activities of Hik14 and WT, we selected the condition under which the difference in growth in the initial phase between WT and Hik14 was still detectable but secondary damaging effects were negligible. For all the subsequent experiments the two strains were cultivated in BG11 medium without Epps buffer, aerated with air enriched with 2% CO_2, and illuminated with light of 60 μmol photons m^{-2} s^{-1}. The inoculation of cells was with an $OD_{750\,nm}$ of 0.1 (referred to as low cell density) or 0.4 (referred to as high cell density), and cells were harvested at the times indicated in the legends to figures and tables (see corresponding growth curves in Fig. 5).

To investigate whether Hik14 has a higher sensitivity towards photoinhibition, the O_2 evolution of intact cells was determined with bicarbonate as electron acceptor under high light illumination (white light of 5,000 μmol photons m^{-2} s^{-1}). Under these conditions the O_2 evolving activity of the mutant was almost as high as that of WT (maximally about 5% lower than that of WT) (not shown). For comparison we measured the O_2 evolving rate of a previously constructed PsbO-free *Synechocystis* PCC 6803 mutant (Engels *et al.*, 1994) which has been shown to be extremely light sensitive (Philbrick *et al.*, 1991). Therefore, the growth deficiency of Hik14 is not due to a higher sensitivity towards photoinhibition as the primary

Table II. Photosynthetic O_2 evolution of *Synechocystis* PCC 6803 WT and mutant Hik14. *Synechocystis* cells were cultivated in BG11 medium (without additional Epps buffer), aerated with air enriched with 2% CO_2, and illuminated with light of 60 μmol photons m^{-2} s^{-1}. Two-day-old cells were inoculated with a cell density of $OD_{750\,nm}$ of 0.1 and cultivated for 48 h, 72 h, and 96 h. Photosynthetic O_2 evolution of intact cells was determined with $NaHCO_3$ and an illumination with red light of 200 μmol photons m^{-2} s^{-1}. The O_2 evolving activity is given per mL cell suspension (CS) and per mg Chl. The unit "mL CS" corresponds to a concentrated cell suspension with $OD_{750\,nm}$ = 100. These results are representative of three independent experiments.

	Growth	Chlorophyll content	Photosynthetic O_2 evolution $H_2O \rightarrow NaHCO_3$	
	$OD_{750\,nm}$	[mg mL CS^{-1}]	[μmol O_2 mL CS^{-1} h^{-1}]	[μmol O_2 mg Chl^{-1} h^{-1}]
Growth for 48 h				
WT	0.81	0.38	87.5	231.2
Hik14	0.51	0.42	81.7	193.5
Growth for 72 h				
WT	1.18	0.49	106.5	209.9
Hik14	0.64	0.39	57.9	149.0
Growth for 96 h				
WT	1.92	0.46	107.7	232.6
Hik14	0.76	0.32	42.9	135.8

reason, although secondary damaging effects can not be excluded. In this respect the Hik14 mutant is different from the DspA-free S*ynechocystis* sp. PCC 6803 mutant (called Hik33) which is severely light sensitive (Grossman *et al.*, 2001; Hsiao *et al.*, 2004; Murata and Suzuki, 2006). DspA (Sll0698) is a global regulator that responds to multiple kinds of stress and helps to coordinate cellular metabolism with growth limitations imposed by the environment (Mikami *et al.*, 2002; Murata and Suzuki, 2006; Tu *et al.*, 2004).

The O_2 evolving activity with bicarbonate of *Synechocystis* PCC 6803 cells which were inoculated at a low density and grown for 48 h, 72 h or 96 h (Table II) was measured. Up to 48 h, WT and Hik14 cells had about equal photosynthetic O_2 evolution. After 72 h and 96 h, the activity of the mutant cells was lower than that of WT, indicating that the cells suffer from some type of metabolic limitation leading eventually to a lower photosynthetic O_2 evolving activity.

A slightly poorer photosynthetic capacity of the mutant cells inoculated with the low cell density could also be detected by determining the pigment fluorescence at 77 K. Hik14 had higher phycocyanobilin fluorescence at 77 K than WT, when inoculated with the low cell density, suggesting again that the mutant suffers from some type of stress in the initial growth phase (not shown). There were no significant differences in the Chl a and phycocyanobilin fluorescence at 77 K between WT

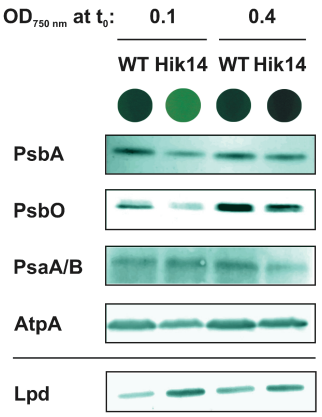

Fig. 6. Immuno blot analyses of selected proteins of *Synechocystis* PCC 6803 WT and mutant Hik14. *Synechocystis* cells were cultivated in BG11 medium (without additional Epps buffer), aerated with air enriched with 2% CO_2, and illuminated with light of 60 μmol photons m^{-2} s^{-1}. Two-day-old cells were inoculated with an $OD_{750\,nm}$ of 0.1 or 0.4 and grown for 48 h (for the corresponding growth curves see Fig. 5). 5 μg protein (for Lpd) or 20 μg protein (for PsbA, PsbO, PsaA/B, and AtpA) were loaded onto the gel. Detection was with the antisera against Lpd, PsbA, PsbO, PsaA/B, and AtpA. The lanes from left to right correspond to: WT, inoculated with an $OD_{750\,nm}$ of 0.1 ($t_{48\,h}$ $OD_{750\,nm}$ = 0.828 and 2.7 μg Chl mL^{-1} medium); Hik14, inoculated with an $OD_{750\,nm}$ of 0.1 ($t_{48\,h}$ $OD_{750\,nm}$ = 0.405 and 1.3 μg Chl mL^{-1} medium); WT, inoculated with an $OD_{750\,nm}$ of 0.4 ($t_{48\,h}$ $OD_{750\,nm}$ = 1.512 and 6.8 μg Chl mL^{-1} medium); Hik14, inoculated with an $OD_{750\,nm}$ of 0.4 ($t_{48\,h}$ $OD_{750\,nm}$ = 1.803 and 8.2 μg Chl mL^{-1} medium). The appearance of the cells is also given.

and Hik14 when inoculated with the high cell density.

To detect molecular changes, levels of selected proteins involved in photosynthesis were compared. Immuno blot analyses (Fig. 6) detected a slightly lower amount of the PS II reaction center protein PsbA and a significant lower amount of the manganese-stabilizing protein PsbO in Hik14 compared to WT when cells were inoculated with the low cell density being consistent with a lower photosynthetic O_2 evolution (Table II).

Analysis of steady state mRNA transcript pools for subunits of the NDH-1 complexes and for PetH in WT and Hik14

Since a drop of pH in the BG11 medium below pH 6.8 shifts the CO_2/HCO_3^- equilibrium in favor of CO_2 (pK 6.8), an up-regulation of the specialized NDH-1B complexes (containing the NdhD3 or NdhD4 but not the NdhD1 or NdhD2 subunits) and of the cyclic electron flow around PS I are expected. These activities are required for the intracellular conversion of CO_2 to HCO_3^- (Badger and Price, 2003; Kaplan and Reinhold, 1999; Price *et al.*, 2002; Shibata *et al.*, 2002). Thus, as a consequence of the pH decrease in the medium profound alterations in the carbon assimilation systems and in the ion pumps (Kaplan *et al.*, 1989; Ogawa and Kaplan, 1987; Wang *et al.*, 2002) as well as in the activities of the electron transport chains in the cytoplasmic and thylakoid membrane are necessary (see Teuber *et al.*, 2001 for a summary of H^+ flux in cyanobacteria).

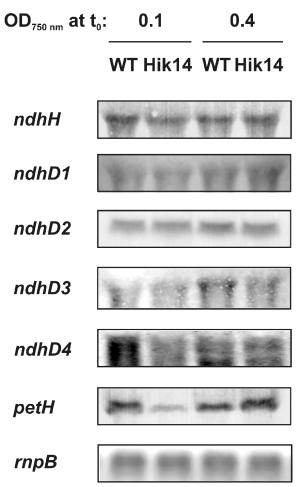

Fig. 7. Northern blot analyses of selected transcripts of *Synechocystis* PCC 6803 WT and mutant Hik14. *Synechocystis* cells were cultivated as given in Fig. 6. The mRNA levels are shown for *ndhH* (encoding the subunit NdhH of the NDH-1 complex of type A and B), *ndhD1* and *ndhD2* (encoding subunits of the NDH-1A complexes), *ndhD3* and *ndhD4* (encoding subunits of the NDH-1B complexes) as well as for *petH* (encoding the ferredoxin:NADP oxidoreductase). Samples from left to right are the same as in Fig. 6.

The Northern blot analyses (Fig. 7) document that Hik14, when inoculated with the low cell density, has a significantly lower transcript level for the NdhD4 subunit of one of the NDH-1B complexes than WT, while the transcript levels for the subunits NdhD1 and NdhD2 of the NDH-1A complexes, not being directly involved in this conversion, were about equal. Furthermore, the amount of transcript for the ferredoxin:NADP oxidoreductase (PetH) was significantly lower in Hik14 as compared to WT. PetH is involved at least in one of the cyclic electron transport routes. Both results suggest that Hik14 is less able than WT to rapidly up-regulate the conversion of CO_2 to HCO_3^- when diluted into fresh BG11 medium at a low cell density and when the pH drop makes it necessary that cells optimize CO_2 assimilation relative to HCO_3^- assimilation. This difference between Hik14 and WT for the transcript level of the NdhD4 subunit of one of the NDH-1B complexes and of PetH was not seen when cells were inoculated with the high cell density.

Analysis of selected metabolites

To uncover possible metabolic limitations in Hik14 cells more globally, a metabolic analysis of hydrophilic substances including sugars, amino acids, and carbonic acids was performed as previously described (Barsch *et al.*, 2004), and the results of four independent growth experiments are given in Table III. A significant and reproducible difference between Hik14 and WT was observed for pyruvate (Hik14 having 36 to 55% of the WT level). This difference was not seen when cells were inoculated with the high cell density. This result prompted us to investigate the level of the dihydrolipoamide dehydrogenase (Lpd), the E3 subunit of the pyruvate dehydrogenase.

An immuno blot analysis showed that the protein level of the Lpd was significantly higher in Hik14 than in WT, especially when cells were inoculated with the low cell density but also when inoculated with the high cell density (Fig. 6). The

Table III. Determination of the relative concentrations of L-glutamate and pyruvate of *Synechocystis* PCC 6803 WT and mutant Hik14. *Synechocystis* cells were cultivated in BG11 medium (without additional Epps buffer), aerated with air enriched with 2% CO_2, and illuminated with light of 60 μmol photons m^{-2} s^{-1}. Two-day-old cells were inoculated with a cell density of $OD_{750\,nm}$ of 0.1 or 0.4 and then cultivated for 48 h. The results of four similar but independent growth experiments are presented.

	$OD_{750\,nm}$			
	$t_0 = 0.1$		$t_0 = 0.4$	
	WT	Hik14	WT	Hik14
	L-Glutamate concentration [rel. units]			
1st Experiment	31	3	60	98
2nd Experiment	130	82	116	116
3rd Experiment	31	1	–	–
4th Experiment	106	1	–	–
	Pyruvate concentration [rel. units]			
1st Experiment	1.2	0.7	1.0	1.1
2nd Experiment	0.9	0.4	0.9	0.9
3rd Experiment	0.5	0.2	–	–
4th Experiment	0.4	0.2	–	–

Lpd represents the E3 subunit of the pyruvate dehydrogenase complex which is mainly associated with the cytoplasmic membrane in *Synechocystis* PCC 6803 (Engels *et al.*, 1997). This suggests that the amount of the cytoplasmic membrane located pyruvate dehydrogenase complex is higher in the mutant leading to a lower pyruvate concentration in Hik14.

The reduced growth of Hik14 in the initial growth phase as compared to WT, when inoculated with the low cell density, also led to a lower glutamate level in Hik14 than in WT. Again, when cells were inoculated with the high cell density, no significant difference of the glutamate level between WT and Hik14 was observed. The substantially higher amount of glutamate in WT as compared to Hik14 was observed in three of the four experiments listed in Table III, while in one experiment the glutamate level was only about twice as high in WT as in Hik14, suggesting that in this experiment the Hik14 cells had already reached the recovery phase (see growth curves in Fig. 5).

Concluding Remarks

Although we can not yet state which are the direct targets for this Slr1759-Slr1760 two-component system, our results provide evidence that it plays a rather complex role in the coordination of photosynthesis, respiration, carbon assimilation, and pH homeostasis. This is in good agreement with the fact that the histidine kinase Slr1759 is cytoplasmic membrane-associated, has a very complex domain structure, and contains a potentially redox active cofactor being FAD as preliminary results have indicated (Michel *et al.*, 2005).

Acknowledgements

The financial support of the Deutsche Forschungsgemeinschaft DFG (FOR387) is gratefully acknowledged. A. B. received a grant from the International NRW Graduate School in Bioinformatics and Genome Research. We thank Dr. Frank Vorhölter, Lehrstuhl für Genetik, Universität Bielefeld, Germany, for his help with bioinformatic tools, Dr. Jochen Kruip, Lehrstuhl für Biochemie der Pflanzen, Ruhr-Universität Bochum, Germany, for a kind gift of the PsaA/B antiserum, and Prof. Dr. Martin Hagemann, Pflanzenphysiologie, Universität Rostock, Germany, for sending us the Hik14 mutant originating from the laboratory of Prof. Dr. Norio Murata, National Institute for Basic Biology, Okazaki, Japan.

Anantharaman V. and Aravind L. (2001), The CHASE domain: a predicted ligand-binding module in plant cytokinin receptors and other eukaryotic and bacterial receptors. Trends Biochem. Sci. **26**, 579–582.

Appleby J. L., Parkinson J. S., and Bourret R. B. (1996), Signal transduction via the multi-step phosphorelay: Not necessarily a road less traveled. Cell **86**, 845–848.

Badger M. R. and Price G. D. (2003), CO2 concentrating mechanisms in cyanobacteria: molecular components, their diversity and evolution. J. Exp. Bot. **54**, 609–622.

Badger M. R., Hanson D., and Price G. D. (2002), Evolution and diversity of CO2 concentrating mechanisms in cyanobacteria. Funct. Plant Biol. **29**, 161–173.

Barsch A., Patschkowski T., and Niehaus K. (2004), Comprehensive metabolite profiling of *Sinorhizobium meliloti* using gas chromatography-mass spectrometry. Funct. Integr. Genomics **4**, 219–230.

Berger S., Ellersiek U., Kinzelt D., and Steinmüller K. (1993), Immunopurification of a subcomplex of the NAD(P)H-plastoquinone-oxidoreductase from the

cyanobacterium *Synechocystis* sp. PCC 6803. FEBS Lett. **326**, 249–250.

Chang C. and Stewart R. C. (1998), The two-component system. Regulation of diverse signaling pathways in prokaryotes and eukaryotes. Plant Physiol. **117**, 723–731.

Engels A., Kahmann U., Ruppel H. G., and Pistorius E. K. (1997), Isolation, partial characterization and localization of a dihydrolipoamide dehydrogenase from the cyanobacterium *Synechocystis* PCC 6803. Biochim. Biophys. Acta **1340**, 33–44.

Engels D. H., Lott A., Schmid G. H., and Pistorius E. K. (1994), Inactivation of the water-oxidizing enzyme in manganese stabilizing protein-free mutant cells of the cyanobacteria *Synechococcus* PCC 7942 and *Synechocystis* PCC 6803 during dark incubation and conditions leading to photoactivation. Photosynth. Res. **42**, 227–244.

Friedrich T. and Scheide D. (2000), The respiratory complex I of bacteria, archaea and eukarya and its module common with membrane-bound multisubunit hydrogenases. FEBS Lett. **479**, 1–5.

Galperin M. Y. (2004), Bacterial signal transduction network in a genomic perspective. Environ. Microbiol. **6**, 552–567.

Grossman A. R., Bhaya D., and He Q. (2001), Tracking the light environment by cyanobacteria and the dynamic nature of light harvesting. J. Biol. Chem. **276**, 11449–11452.

Herranen M., Battchikova N., Zhang P., Graf A., Sirpio S., Paakkarinen V., and Aro E. M. (2004), Towards functional proteomics of membrane protein complexes in *Synechocystis* sp. PCC 6803. Plant Physiol. **134**, 470–481.

Hirano M., Satoh K., and Katoh S. (1980), Plastoquinone as a common link between photosynthesis and respiration in blue-green alga. Photosynth. Res. **1**, 149–162.

Howitt C. A., Cooley J. W., Wiskich J. T., and Vermaas W. F. (2001), A strain of *Synechocystis* sp. PCC 6803 without photosynthetic oxygen evolution and respiratory oxygen consumption: implications for the study of cyclic photosynthetic electron transport. Planta **214**, 46–56.

Hsiao H. Y., He Q., Van Waasbergen L. G., and Grossman A. R. (2004), Control of photosynthetic and high-light-responsive genes by the histidine kinase DspA: negative and positive regulation and interactions between signal transduction pathways. J. Bacteriol. **186**, 3882–3888.

Kaneko T., Sato S., Kotani H., Tanaka A., Asamizu E., Nakamura Y., Miyajima N., Hirosawa M., Sugiura M., Sasamoto S., Kimura T., Hosouchi T., Matsuno A., Muraki A., Nakazaki N., Naruo K., Okumura S., Shimpo S., Takeuchi C., Wada T., Watanabe A., Yamada M., Yasuda M., and Tabata S. (1996), Sequence analysis of the genome of the unicellular cyanobacterium *Synechocystis* sp. strain PCC 6803. II. Sequence determination of the entire genome and assignment of potential protein-coding regions (supplement). DNA Res. **3**, 185–209.

Kaneko T., Nakamura Y., Sasamoto S., Watanabe A., Kohara M., Matsumoto M., Shimpo S., Yamada M., and Tabata S. (2003), Structural analysis of four large plasmids harboring in a unicellular cyanobacterium, *Synechocystis* sp. PCC 6803. DNA Res. **10**, 221–228.

Kaneko T., Sato S., Nakamura Y., and Tabata S. (2005), Large scale analysis of protein-protein interactions in *Synechocystis* sp. PCC 6803 using a YTH system. In: 3rd Japan-German Joint Seminar: Functional Genomics of Cyanobacteria. New Approaches for Investigation of Diversity (Tabata S., ed.). Tomiura, Chiba, Japan, pp. 12–13.

Kaplan A. and Reinhold L. (1999), CO2 concentrating mechanisms in photosynthetic microorganisms. Annu. Rev. Plant Physiol. Plant Mol. Biol. **50**, 539–570.

Kaplan A., Scherer S., and Lerner M. (1989), Nature of high-light induced H^+-efflux and Na^+ uptake in cyanobacteria. Plant Physiol. **89**, 1220–1225.

Matsushika A. and Mizuno T. (1998), A dual-signaling mechanism mediated by the ArcB hybrid sensor kinase containing the histidine-containing phosphotransfer domain in *Escherichia coli*. J. Bacteriol. **180**, 3973–3977.

Matthijs H. C., Jeanjean R., Yeremenko N., Huiwman J., Joset F., and Hellingwerf K. J. (2002), Hypothesis: versatile function of ferredoxin-NADP+ reductase in cyanobacteria provides regulation for transient photosystem I-driven cyclic electron transport. Funct. Plant Biol. **29**, 201–210.

Meunier P. C., Colon-Lopez M. S., and Sherman L. A. (1997), Temporal changes in state transitions and photosystem organization in the unicellular, diazotrophic cyanobacterium *Cyanothece* sp. ATCC 51142. Plant Physiol. **115**, 991–1000.

Michel K. P., Thole H. H., and Pistorius E. K. (1996), IdiA, a 34 kDa protein in the cyanobacteria *Synechococcus* sp. strains PCC 6301 and PCC 7942, is required for growth under iron and manganese limitations. Microbiology **142**, 2635–2645.

Michel K. P., Krüger F., Pühler A., and Pistorius E. K. (1999), Molecular characterization of *idiA* and adjacent genes in the cyanobacteria *Synechococcus* sp. strains PCC 6301 and PCC 7942. Microbiology **145**, 1473–1484.

Michel K.-P., Nodop A., Suzuki I., Staiger D., and Pistorius E. K. (2005), Comparative analyses of *Synechocystis* sp. PCC 6803 wild type and the histidine kinase Slr1759-free mutant Hik14. In: 3rd Japan-German Joint Seminar: Functional Genomics of Cyanobacteria. New Approaches for Investigation of Diversity (Tabata S., ed.). Tomiura, Chiba, Japan, pp. 52–53.

Mikami K., Kanesaki Y., Suzuki I., and Murata N. (2002), The histidine kinase Hik33 perceives osmotic stress and cold stress in *Synechocystis* sp. PCC 6803. Mol. Microbiol. **46**, 905–915.

Mizuno T., Kaneko T., and Tabata S. (1996), Compilation of all genes encoding bacterial two-component signal transducers in the genome of the cyanobacterium *Synechocystis* sp. strain PCC 6803. DNA Res. **3**, 407–414.

Mougel C. and Zhulin I. B. (2001), CHASE: an extracellular sensing domain common to transmembrane receptors from prokaryotes, lower eukaryotes and plants. Trends Biochem. Sci. **26**, 582–584.

Mullineaux C. W. and Allen F. (1990), State 1-State 2 transitions in the cyanobacterium *Synechococcus* 6301 are controlled by the redox state of electron carriers

between photosystem I and II. Photosynth. Res. **23**, 297–311.

Murata N. and Suzuki I. (2006), Exploitation of genomic sequences in a systematic analysis to access how cyanobacteria sense environmental stress. J. Exp. Bot. **57**, 235–247.

Ogawa T. and Kaplan A. (1987), The stoichiometry between CO2 and H+ fluxes involved in the transport of inorganic carbon in cyanobacteria. Plant Physiol. **83**, 888–891.

Ogawa T. and Kaplan A (2003), Inorganic carbon acquisition systems in cyanobacteria. Photosynth. Res. **77**, 105–115.

Ohkawa H., Pakrasi H. B., and Ogawa T. (2000), Two types of functionally distinct NAD(P)H dehydrogenases in *Synechocystis* sp. strain PCC 6803. J. Biol. Chem. **275**, 31630–31634.

Ohkawa H., Sonoda M., Shibata M., and Ogawa T. (2001), Localization of NAD(P)H dehydrogenase in the cyanobacterium *Synechocystis* sp. strain PCC 6803. J. Bacteriol. **183**, 4938–4939.

Ohkawa H., Sonoda M., Hagino N., Shibata M., Pakrasi H. B., and Ogawa T. (2002), Functionally distinct NAD(P)H dehydrogenases and their membrane localization in *Synechocystis* sp. PCC 6803. Funct. Plant Biol. **29**, 195–200.

Omata T. and Murata N. (1984), Isolation and characterization of three types of membranes from the cyanobacterium *Synechocystis* PCC 6714. Arch. Microbiol. **139**, 113–116.

Pernestig A. K., Georgellis D., Romeo T., Suzuki K., Tomenius H., Normark S., and Melefors O. (2003), The *Escherichia coli* BarA-UvrY two-component system is needed for efficient switching between glycolytic and gluconeogenic carbon sources. J. Bacteriol. **185**, 843–853.

Philbrick J. B., Diner B. A., and Zilinskas B. A. (1991), Construction and characterization of cyanobacterial mutants lacking the manganese-stabilizing polypeptide of photosystem II. J. Biol. Chem. **266**, 13370–13376.

Price G. D., Maeda S., Omata T., and Badger M. R. (2002), Modes of active inorganic carbon uptake in the cyanobacterium *Synechococcus* sp. PCC 7942. Funct. Plant Biol. **29**, 131–149.

Prommeenate P., Lennon A. M., Markert C., Hippler M., and Nixon P. J. (2004), Subunit composition of NDH-1 complexes of *Synechocystis* sp. PCC 6803: identification of two new *ndh* gene products with nuclear-encoded homologues in the chloroplast Ndh complex. J. Biol. Chem. **279**, 28165–28173.

Reddy K. J., Webb R., and Sherman L. A. (1990), Bacterial RNA isolation with one hour centrifugation in a table-top ultracentrifuge. BioTechniques **8**, 250–251.

Shibata M., Ohkawa H., Katoh H., Shimoyama M., and Ogawa T. (2002), Two CO2 uptake system in cyanobacteria: Four systems for inorganic carbon acquisition in *Synechocystis* sp. strain PCC 6803. Funct. Plant Biol. **29**, 123–129.

Stephan D. P., Ruppel H. G., and Pistorius E. K. (2000), Interrelation between cyanophycin synthesis, L-arginine catabolism and photosynthesis in the cyanobacterium *Synechocystis* sp. strain PCC 6803. Z. Naturforsch. **55c**, 927–942.

Stock A. M., Robinson V. L., and Goudreau P. N. (2000), Two-component signal transduction. Annu. Rev. Biochem. **69**, 183–215.

Suzuki I., Los D. A., Kanesaki Y., Mikami K., and Murata N. (2000), The pathway for perception and transduction of low-temperature signals in *Synechocystis*. Embo J. **19**, 1327–1334.

Taylor B. L. and Zhulin I. B. (1999), PAS domains: Internal sensors of oxygen, redox potential, and light. Microbiol. Mol. Biol. Rev. **63**, 479–506.

Teuber M., Rogner M., and Berry S. (2001), Fluorescent probes for non-invasive bioenergetic studies of whole cyanobacterial cells. Biochim. Biophys. Acta **1506**, 31–46.

Tölle J., Michel K. P., Kruip J., Kahmann U., Preisfeld A., and Pistorius E. K. (2002), Localization and function of the IdiA homologue Slr1295 in the cyanobacterium *Synechocystis* sp. strain PCC 6803. Microbiology **148**, 3293–3305.

Tu C. J., Shrager J., Burnap R. L., Postier B. L., and Grossman A. R. (2004), Consequences of a deletion in *dspA* on transcript accumulation in *Synechocystis* sp. strain PCC 6803. J. Bacteriol. **186**, 3889–3902.

Vermaas W. F. J. (2001), Photosynthesis and respiration in cyanobacteria. In: Encyclopedia of Life Sciences. Nature Publishing Group, London, pp. 1–7.

Wang H. L., Postier B. L., and Burnap R. L. (2002), Polymerase chain reaction-based mutageneses identify key transporters belonging to multigene families involved in Na+ and pH homeostasis of *Synechocystis* sp. PCC 6803. Mol. Microbiol. **44**, 1493–1506.

West A. H. and Stock A. M. (2001), Histidine kinases and response regulator proteins in two-component signaling systems. Trends Biochem. Sci. **26**, 369–376.

Yeremenko N., Jeanjean R., Prommeenate P., Krasikov V., Nixon P. J., Vermaas W. F., Havaux M., and Matthijs H. C. (2005), Open reading frame *ssr2016* is required for antimycin A-sensitive photosystem I-driven cyclic electron flow in the cyanobacterium *Synechocystis* sp. PCC 6803. Plant Cell Physiol. **46**, 1433–1436.

Zhulin I. B. and Taylor B. L. (1998), Correlation of PAS domains with electron transport-associated proteins in completely sequenced microbial genomes. Mol. Microbiol. **29**, 1522–1523.

Zhulin I. B., Taylor B. L., and Dixon R. (1997), PAS domain S-boxes in Archaea, Bacteria and sensors for oxygen and redox. Trends Biochem. Sci. **22**, 331–333.

Zhulin I. B., Nikolskaya A. N., and Galperin M. Y. (2003), Common extracellular sensory domains in transmembrane receptors for diverse signal transduction pathways in bacteria and archaea. J. Bacteriol. **185**, 285–294.